JACS
JOURNAL OF THE AMERICAN CHEMICAL SOCIETY
pubs.acs.org/JACS
Communication

Five Nitrogen Oxidation States from Nitro to Amine: Stabilization and Reactivity of a Metastable Arylhydroxylamine Complex

Joseph Zsombor-Pindera,[§] Farshid Effaty,[§] Léon Escomel, Brian Patrick, Pierre Kennepohl,* and Xavier Ottenwaelder*

Cite This: https://dx.doi.org/10.1021/jacs.0c09300
Read Online
ACCESS | Metrics & More | Article Recommendations | Supporting Information

ABSTRACT: Redox noninnocent ligands enhance the reactivity of the metal they complex, a strategy used by metalloenzymes and in catalysis. Herein, we report a series of copper complexes with the same ligand framework, but with a pendant nitrogen group that spans five different redox states between nitro and amine. Of particular interest is the synthesis of a unprecedented copper(I)-arylhydroxylamine complex. While hydroxylamines typically disproportionate or decompose in the presence of transition metal ions, the reactivity of this metastable species is arrested by the presence of an intramolecular hydrogen bond. Two-electron oxidation yields a copper(II)-(arylnitrosyl radical) complex that can dissociate to a copper(I) species with uncoordinated arylnitroso. This combination of ligand redox noninnocence and hemilability provides opportunities in catalysis for two-electron chemistry via a one-electron copper(I/II) shuttle, as exemplified with an aerobic alcohol oxidation.

The chemistry of aromatic primary hydroxylamines (Ar−NH−OH) and nitrosoarenes (Ar−N═O) is of considerable interest due to their inherent reactivity, redox properties, implication in biological processes, and involvement in catalytic transformations. While these reactive compounds often trigger deleterious effects on the body (DNA mutations, protein adducts), they are relevant as more stable analogues of NH_2OH and HNO to study pathways germane to the production of nitric oxide (NO), nitrous oxide (N_2O) and derivatives.[1−5] In synthesis, the relatively weak N−O bond of hydroxylamines (BDEs: H_2N−OH = 214 kJ/mol vs C−N/O > 300 kJ/mol) and the electrophilic properties of nitroso compounds led to the development of catalytic reactions for C−N and C−O bond formation.[6−9]

In these catalytic systems, the reactivity of ArNHOH and ArNO species is controlled by transition metal ions (M), notably earth-abundant Fe and Cu. The redox noninnocence of ArNO when bonded to metal ions generates M/ArNO adducts[10−23] that mimic the geometry and electronic structure of M/O_2 adducts found in oxygenases[24−27] and oxidative catalysis.[28] By contrast, ArNHOH is quite reactive in the presence of metal ions. Only a few examples of metal complexes exist with chelating *alkyl*hydroxylamines.[29−31] Employing *aryl*hydroxylamines typically leads to disproportionation[6−8,32−35] or decomposition[36] of ArNHOH. This explains the dearth of data regarding metal-mediated hydroxylamine-based reactions. For example, how is the two-electron conversion between ArNHOH and ArNO performed with a one-electron shuttle such as Cu^{II}/Cu^{I} during catalytic transformations?[6−8]

In this work, we report an intramolecular strategy to overcome these challenges and control the chemistry of redox noninnocent ArNHOH with metal ions (Scheme 1). We prepared a multidentate ligand containing a primary arylhydroxylamine function that acts as a pro-ligand for chelated metal-ArNO species. With this design, we obtained the first structurally confirmed arylhydroxylamine complex (**1**), studied its two-electron oxidation (to complex **2**), and used it in a catalytic two-electron organic oxidation.

Scheme 1

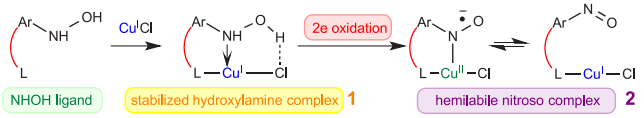

Hydroxylamine-containing ligand L^{NHOH} (Scheme 2) was synthesized by a carefully monitored partial reduction of L^{NO2} over zinc (SI Section 1c). Varying the reaction time and quantity of reductant allowed us to obtain samples of all three accessible oxidation states, L^{NO2}, L^{NHOH}, and L^{NH2} (Scheme 2). Ligands L^{NO2} and L^{NH2}, with the most stable nitrogen oxidation states, form standard copper complexes. This is illustrated by [L^{NO2}CuCl] and [L^{NH2}CuCl], observed as (μ-$Cl)_2Cu_2$ dimers in the crystalline state (Scheme 2a, Figure S9).

As an intermediate oxidation state between L^{NO2} and L^{NH2}, L^{NHOH} is poised for reactivity with a redox-active metal ion. Indeed, reaction of L^{NHOH} with [$Cu^{I}(CH_3CN)_4$](X) (X^- = PF_6^- or $CF_3SO_3^-$) led to a purple solution (λ_{max} = 508 nm with a shoulder at 650 nm) that contained products of the disproportionation of L^{NHOH}, [L^{NO}Cu]$^+$ and [L^{NH2}Cu]$^+$, as shown by ESI-MS (Scheme 2b, Figure S5). Reaction of L^{NHOH}

Received: August 29, 2020

Scheme 2. (a) Coordination of L^{NO2} and L^{NH2} with CuCl; (b) Disproportionation of L^{NHOH} with $[Cu(CH_3CN)_4]PF_6$; (c) Capture of L^{NHOH} by CuCl Leading to $[L^{NHOH}CuCl]$ (1)

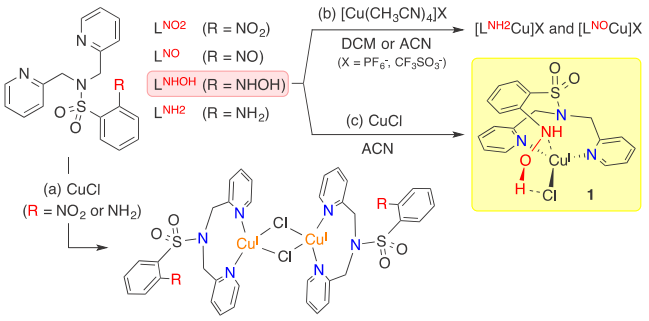

with $Cu^{I}Cl$, however, led to a single well-defined species, $[L^{NHOH}CuCl]$ (**1**), which precipitates as a yellow powder in 75% yield (Scheme 2c). X-ray diffraction analysis of **1** shows a Cu^{I} center in a T-shape geometry interacting weakly with the ArNHOH (Cu···N1 = 2.657 Å) and the sulfonanide (Cu···N2 = 2.673 Å) (Figure 1). **1** constitutes a very rare case of a

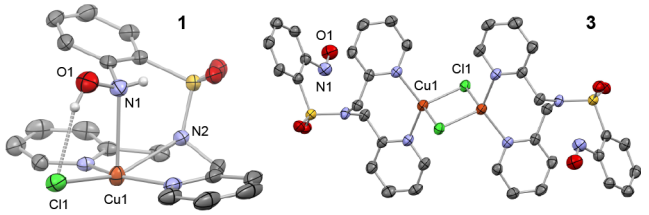

Figure 1. ORTEP view with 50% probability ellipsoids of **1** and **3**. Solvent molecules and H atoms were omitted for clarity, except those on the NHOH function of **1**.

complex with an intact primary hydroxylamine ligand (N1−O1 = 1.418 Å)[29−31] (some examples also exist with a ligated $ArNHO^{-}$ moiety[18,20] or secondary aminoxyl[37] groups). Close inspection reveals that the OH group is involved in a hydrogen bond with the Cl atom (O···Cl = 3.094 Å), possibly explaining the unusual stability of this ArNHOH moiety.

The relative stability of complex **1** provides a unique opportunity to access the L^{NO} complex by 2*e* oxidation and thus complete the nitrogen oxidation state series (Scheme 2). Oxidation of **1** by diethyl or diisopropyl azadicarboxylate (DEAD or DIAD) led to the formation a *deep-purple* complex (λ_{max} = 508 nm, ε_{508} = 2450 M^{-1} cm^{-1}), $[L^{NO}CuCl]$, **2** (Scheme 3a). Titration of **1** with DEAD in dichloromethane (DCM) reached maximum absorbance at 2.0 equiv, suggesting

Scheme 3. (a) Oxidation of 1 by DEAD or DIAD to Form 2; (b) Dimerization to 3 upon Crystallization

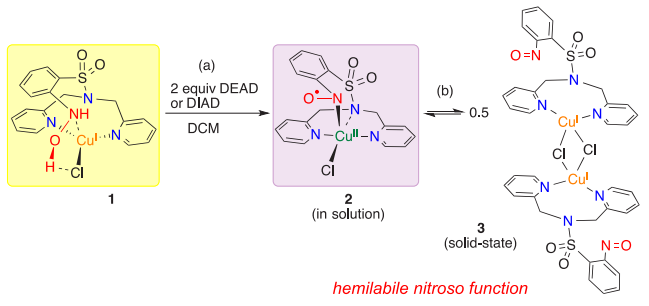

that DEAD acts as a single hydrogen atom abstractor (Figure S10).[38] Species **2** was characterized in solution by ESI-MS (*m*/*z* = 431.1 for $L^{NO}Cu^{+}$, Figure S11), displays broadened ^{1}H NMR peaks in $CDCl_3$ (Figure S12), and is EPR-silent in frozen DCM solution at 77 K. Diffusion of pentane into a −30 °C DCM solution of **2** produced by oxidation with DEAD yielded *light-red* crystals. X-ray diffraction of these crystals revealed that **2** dimerizes in the solid state as a $(\mu\text{-Cl})_2Cu_2$ complex, $[L^{NO}CuCl]_2$, **3**, in which the ArNO moiety is not coordinated (Figure 1) and remains a double-bonded $(ArNO)^0$ (N1−O1 = 1.236 Å).[39]

Given the redox noninnocence of ArNO species, two electromers are possible for **2**: $[(L^{NO})^0Cu^{I}Cl]$, with an N═O double bond, and $[(L^{NO\bullet-})Cu^{II}Cl]$, an arylnitrosyl π-radical with an N−O bond order of 1.5. Evans ^{1}H NMR measurements on solutions of **2** indicated paramagnetism with $\chi_M T \approx 0.13$ emu K mol^{-1} (Figure S12), well below the expected value for two individual 1/2 spins (0.75 emu K mol^{-1}), which strongly suggests that **2** is an antiferromagnetically coupled Cu^{II}-radical species. The electronic structure of **2** was also explored by Cu K-edge X-ray absorption spectroscopy (XAS, Figure 3, SI Section 6). The Cu K-edge XAS of **1** (15 mM in frozen DCM or in the solid state) is consistent with Cu^{I}, with a prominent edge feature at 8985.8 eV ascribed to the characteristic Cu^{I} 4p ← 1s peak.[40,41] The Cu K-edge XAS of **2** (made with 3 equiv of DIAD, 15 mM in frozen DCM solution), on the other hand, exhibits features more characteristic of a Cu^{II} species, with an edge at 8985.0 eV, shifted 2.2 eV with respect to that of **1**, and a weak low-energy Cu 3d ← 1s pre-edge feature at 8977.6 eV.[40]

DFT and EXAFS data support that the $(ArNO)^{\bullet-}$ moiety in **2** is coordinated to Cu^{II} in a κN fashion. DFT calculations at the CAM-B3LYP/Def2-TZVP level of theory (SI Section 8) on **2** predict a distorted square-pyramidal coordination geometry and a κN-$(ArNO)^{\bullet-}$ moiety having a NO bond length of 1.28 Å (Figure 4). The antiferromagnetically coupled singlet (^{1}**2**) and ferromagnetically coupled triplet (^{3}**2**) are predicted to be nearly isoenergetic (Table S15). TD-DFT calculations yield good agreements with the experimental XAS (Figures S24−S26) and UV−vis (Figure S27) spectra. The 508 nm peak in the experimental UV−vis spectrum of **2** can be assigned as a ligand-to-metal charge transfer from the $(ArNO)^{\bullet-}$ π system to the Cu^{II} d-hole (Figure S28). The same MO assigned as the Cu^{II} d-hole is the acceptor orbital in the Cu 3d ← 1s pre-edge transition state of the TD-DFT-calculated XAS of **2** (Figures S25, S26). Finally, the EXAFS from the Cu K-edge XAS of **2** was fitted by taking the DFT-optimized geometry as initial guess (Figure 4, SI Section 7). The resulting fit (Figure 3, Table S10) is fully consistent with the mononuclear Cu^{II}-κN-$(ArNO)^{\bullet-}$ assignment for **2**.

Following these structural characterizations, we aimed to study the reactivity of complexes **1** and **2**, because they possess the most reactive nitrogen oxidation states within the series of ligands. Complex **1** is metastable and disproportionates upon application of mechanical force (Figure 4a). Grinding a microcrystalline sample of **1** at 30 Hz for 15 min in a mechanochemical ball miller led to an amorphous purple powder (λ_{max} = 508 nm in DCM). ESI-MS analysis (Figure S14) revealed peaks for $[L^{NO}Cu]^{+}$ and $[L^{NH2}Cu]^{+}$, and XAS supports the formation of a mixture of Cu^{I} and Cu^{II} species (Figure 3). Ion metathesis with $NaBAr^{F}_4$ in DCM led to a dark purple/magenta solution, from which dark purple crystals were obtained (Figure 4b,c). X-ray diffraction revealed a dinuclear

https://dx.doi.org/10.1021/jacs.0c09300
J. Am. Chem. Soc. XXXX, XXX, XXX−XXX

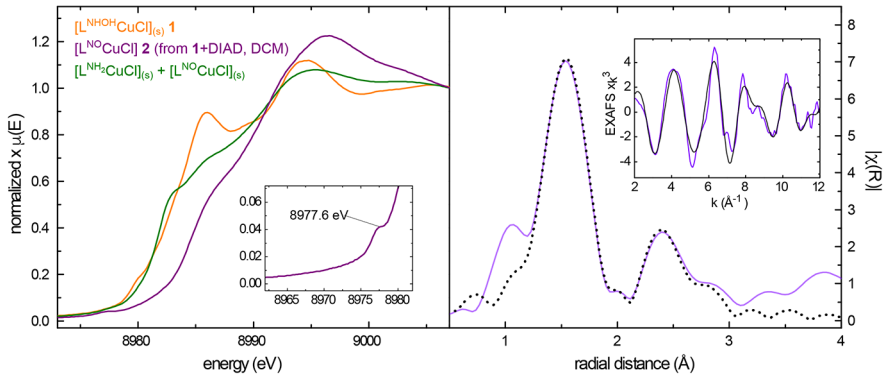

Figure 2. (Left) Cu K-edge X-ray absorbance spectra of **1** (orange), **2** (purple), and the product of mechanochemically induced disproportionation of **1** in the solid state, under N_2 (green). (Right) Fourier transform and k^3-space (inset) of the Cu K-edge EXAFS of a frozen solution of **2** in DCM (purple), showing the best fit (dotted line), performed using a *k*-range of 2−12 $Å^{-1}$ and an *R*-range of 1.1 to 3.1 Å. Fit: 3N at 1.98 Å (N_{py} and N_{NO}), 1Cl of 2.28 Å, 1N at 2.42 Å (N_{SO2}), 1O at 2.61 Å (O_{NO}), 4C at 2.91 Å.

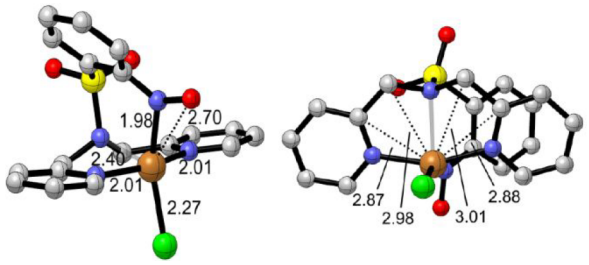

Figure 3. Two views of the DFT model of ^{1}**2**, optimized at the CAM-B3LYP/Def2-TZVP level of theory, showing distances relevant to the EXAFS fit.

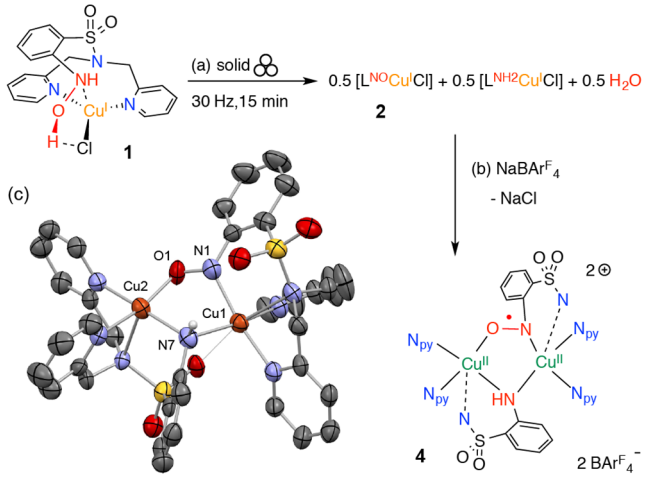

Figure 4. (a) Mechanochemical disproportionation of **1** in plastic jars with a zirconia ball. (b) Dehalogenation to **4** (simplified scheme for clarity). (c) ORTEP view with 50% probability ellipsoids of the dication in **4**. Counterions and hydrogen atoms were omitted for clarity, except the H on the NH^- function.

Cu^{II} complex, $[(\mu\text{-}L^{NO\bullet-})(\mu\text{-}L^{NH-})Cu^{II}_2](BAr^F_4)_2$ (**4**). The Cu−N_{NO} bond to L^{NO} remains intact in a *κN* fashion, with a 1.322 Å N−O bond length consistent with an $(ArNO)^{\bullet-}$ oxidation state.

When complexed, L^{NO} behaves as a hemilabile, redox noninnocent ligand. The crystal structure of **4** confirms that L^{NO} in **2** can bind to Cu^{II} as a *κN*-$(ArNO)^{\bullet-}$, and the crystal structure of **3** shows that L^{NO} can easily dissociate,[17] forming a pendant $(ArNO)^0$ and reducing Cu^{II} back to Cu^{I}. Since $(\mu$-$Cl)_2Cu_2$ dimeric structures similar to **3** were obtained with L^{NH2} and L^{NO2} (Figure S9), this hemilability is a sign of the strong coordinating ability of the ArNO moiety in the L^{NO} ligand.

Facile, reversible ligand exchange due to hemilability is known to enhance reactivity. Based on the 2*e* conversion between **1** and **2**, we therefore attempted a model 2*e*-oxidation reaction, namely the aerobic oxidation of benzyl alcohol (Scheme 4). Bubbling O_2 onto complex **1** in THF led to a

Scheme 4

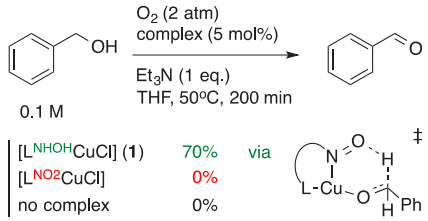

rapid formation of purple compound **2**, highlighting the possibility of using O_2 as terminal oxidant under turnover conditions. Thus, a 70% yield of benzaldehyde was obtained after 200 min at 50 °C using 5 mol % of **1** as precatalyst.

The essential role of the NHOH function in the precatalyst is striking. No turnover was observed when replacing **1** with the similar L^{NO2} complex, in which the NO_2 function is a mere spectator. The NO function is key to turnover, as complex **2** is similar to azo-based[42,43] (Markó) and nitroxide-based[44,45] (TEMPO, DBED) Cu-catalyzed aerobic alcohol oxidation systems. The NO bond in **2** substitutes for the NN bond in Markó's azo precatalyst or the NO nitroxide radical in TEMPO- and DBED-based systems, but in an intramolecular[46] fashion. By analogy, a six-membered transition state can be proposed (Scheme 4).

In conclusion, a single ligand framework has led to a series of crystallographically characterized complexes with a nitrogen pendant group in five oxidation states:[47] $-N^{III}O_2$, $-N^{I}O$ (**3**), $-N^{0}O^{\bullet-}$ (**2**), $-N^{-I}HOH$ (**1**), and $-N^{-III}H_2$. We submit that trapping of an ArNHOH function by inclusion of a good hydrogen bond acceptor adjacent to a metal center can be used as a general strategy for synthesis of complexes of L_nArNO, in which the ArNO can act as a hemilabile[48,49] redox non-innocent[50] ligand. This strategy mimics nature's approach of

https://dx.doi.org/10.1021/jacs.0c09300
J. Am. Chem. Soc. XXXX, XXX, XXX−XXX

coupling earth-abundant metal ions with noninnocent organic cofactors to enable 2*e* processes.[51] The hydrogen bond in **1** also evokes cytochrome P460 activity used by nitrifiers and methanotrophs, where a distal base is required as a proton relay to enable NH_2OH reactivity.[52] The possibility for hemilability in ArNO complexes further expands the range of possible chemical states and makes them attractive candidates for ligand-participatory catalysis, in which ArNOs could act as electron reservoirs, enhancing the oxidative malleability of the metal center.[53]

■ ASSOCIATED CONTENT

Supporting Information

The Supporting Information is available free of charge at https://pubs.acs.org/doi/10.1021/jacs.0c09300.

Experimental details and supporting experiments (PDF)

Crystal information files for CCDC number 1962820 (CIF)

Crystal information files for CCDC number 1962821 (CIF)

Crystal information files for CCDC number 1962822 (CIF)

Crystal information files for CCDC number 1962858 (CIF)

Crystal information files for CCDC number 1962859 (CIF)

■ AUTHOR INFORMATION

Corresponding Authors

Xavier Ottenwaelder − *Department of Chemistry and Biochemistry, Concordia University, Montreal, QC H4B 1R6, Canada;* orcid.org/0000-0003-4775-0303; Email: dr.x@concordia.ca

Pierre Kennepohl − *Department of Chemistry, University of British Columbia, Vancouver, BC V6T 1Z1, Canada;* orcid.org/0000-0003-3408-9157; Email: pierre.kennepohl@ubc.ca, pierre.kennepohl@ucalgary.ca

Authors

Joseph Zsombor-Pindera − *Department of Chemistry and Biochemistry, Concordia University, Montreal, QC H4B 1R6, Canada; Department of Chemistry, University of British Columbia, Vancouver, BC V6T 1Z1, Canada;* orcid.org/0000-0002-9051-1319

Farshid Effaty − *Department of Chemistry and Biochemistry, Concordia University, Montreal, QC H4B 1R6, Canada;* orcid.org/0000-0002-2389-4903

Léon Escomel − *Department of Chemistry and Biochemistry, Concordia University, Montreal, QC H4B 1R6, Canada;* orcid.org/0000-0001-7744-1048

Brian Patrick − *Department of Chemistry, University of British Columbia, Vancouver, BC V6T 1Z1, Canada;* orcid.org/0000-0002-2921-8439

Complete contact information is available at: https://pubs.acs.org/10.1021/jacs.0c09300

Author Contributions

[§]J. Zsombor-Pindera and F. Effaty contributed equally.

Notes

The authors declare no competing financial interest.

■ ACKNOWLEDGMENTS

This work was supported by the Natural Sciences and Engineering Council of Canada (NSERC, Discovery Grants RGPIN-2016-05453 to P.K. and RGPIN-2015-04044 to X.O.). NSERC is acknowledged for an Undergraduate Research Summer Award to J.Z.P. Use of the Stanford Synchrotron Radiation Lightsource, SLAC National Accelerator Laboratory (XAS experiments), is supported by the U.S. Department of Energy, Office of Science, Office of Basic Energy Sciences, under Contract No. DE-AC02-76SF00515. The SSRL Structural Molecular Biology Program is supported by the DOE Office of Biological and Environmental Research and by the National Institutes of Health, National Institute of General Medical Sciences (P41GM103393). The contents of this publication are solely the responsibility of the authors and do not necessarily represent the official views of NIGMS or NIH. We are grateful to the Québec-funded Centre of Green Chemistry and Catalysis for additional resources. We are also grateful to Prof. Tomislav Friščić (McGill), Prof. Louis Cuccia, and Jean-Louis Do (Concordia) for their help with solid-state experiments, and Drs. Casey Van Stappen and Ragnar Björnsson (MPI) for fruitful discussions on EXAFS and computational methodology, respectively.

■ REFERENCES

(1) Kuypers, M. M. M.; Marchant, H. K.; Kartal, B. The microbial nitrogen-cycling network. *Nat. Rev. Microbiol.* **2018**, *16* (5), 263−276.

(2) Flores-Santana, W.; Salmon, D. J.; Donzelli, S.; Switzer, C. H.; Basudhar, D.; Ridnour, L.; Cheng, R.; Glynn, S. A.; Paolocci, N.; Fukuto, J. M.; Miranda, K. M.; Wink, D. A. The Specificity of Nitroxyl Chemistry Is Unique Among Nitrogen Oxides in Biological Systems. *Antioxid. Redox Signaling* **2011**, *14* (9), 1659−1674.

(3) Lehnert, N.; Berto, T. C.; Galinato, M. G. I.; Goodrich, L. E. 63 The Role of Heme-Nitrosyls in the Biosynthesis, Transport, Sensing, and Detoxification of Nitric Oxide (NO) in Biological Systems: Enzymes and Model Complexes. In *Handbook of Porphyrin Science*; Kadish, K. M.; Smith, K. M., Eds.; World Scientific Publishing Company, 2011; Vol. *14*, pp 1−247.

(4) Doctorovich, F.; Bikiel, D. E.; Pellegrino, J.; Suárez, S. A.; Martí, M. A. Reactions of HNO with Metal Porphyrins: Underscoring the Biological Relevance of HNO. *Acc. Chem. Res.* **2014**, *47* (10), 2907−2916.

(5) Abucayon, E. G.; Khade, R. L.; Powell, D. R.; Zhang, Y.; Richter-Addo, G. B. Not Limited to Iron: A Cobalt Heme-NO Model Facilitates N-N Coupling with External NO in the Presence of a Lewis Acid to Generate N_2O. *Angew. Chem., Int. Ed.* **2019**, *58* (51), 18598−18603.

(6) Srivastava, R. S.; Khan, M. A.; Nicholas, K. M. A Novel Intermediate in Allylic Amination Catalyzed by Iron Salts. *J. Am. Chem. Soc.* **1996**, *118* (13), 3311−3312.

(7) Ho, C.-M.; Lau, T.-C. Copper-catalyzed amination of alkenes and ketones by phenylhydroxylamine. *New J. Chem.* **2000**, *24* (11), 859−863.

(8) Srivastava, R. S.; Tarver, N. R.; Nicholas, K. M. Mechanistic Studies of Copper(I)-Catalyzed Allylic Amination. *J. Am. Chem. Soc.* **2007**, *129* (49), 15250−15258.

(9) Cheung, C. W.; Leendert Ploeger, M.; Hu, X. Amide synthesis via nickel-catalysed reductive aminocarbonylation of aryl halides with nitroarenes. *Chem. Sci.* **2018**, *9* (3), 655−659.

(10) Lee, J.; Chen, L.; West, A. H.; Richter-Addo, G. B. Interactions of Organic Nitroso Compounds with Metals. *Chem. Rev.* **2002**, *102* (4), 1019−1066.

(11) Zuman, P.; Shah, B. Addition, Reduction, and Oxidation Reactions of Nitrosobenzene. *Chem. Rev.* **1994**, *94* (6), 1621−1641.

(12) Wiese, S.; Kapoor, P.; Williams, K. D.; Warren, T. H. Nitric Oxide Oxidatively Nitrosylates Ni(I) and Cu(I) C-Organonitroso Adducts. *J. Am. Chem. Soc.* **2009**, *131* (50), 18105−18111.
(13) Labios, L. A.; Millard, M. D.; Rheingold, A. L.; Figueroa, J. S. Bond Activation, Substrate Addition and Catalysis by an Isolable Two-Coordinate Pd(0) Bis-Isocyanide Monomer. *J. Am. Chem. Soc.* **2009**, *131* (32), 11318−11319.
(14) Tomson, N. C.; Labios, L. A.; Weyhermüller, T.; Figueroa, J. S.; Wieghardt, K. Redox Noninnocence of Nitrosoarene Ligands in Transition Metal Complexes. *Inorg. Chem.* **2011**, *50*, 5763−5776.
(15) Askari, M. S.; Girard, B.; Murugesu, M.; Ottenwaelder, X. The two spin states of an end-on copper(II)-superoxide mimic. *Chem. Commun.* **2011**, *47* (28), 8055−8057.
(16) Askari, M. S.; Orio, M.; Ottenwaelder, X. Controlled nitrene transfer from a tyrosinase-like arylnitroso-copper complex. *Chem. Commun.* **2015**, *51* (56), 11206−11209.
(17) Barnett, B. R.; Labios, L. A.; Moore, C. E.; England, J.; Rheingold, A. L.; Wieghardt, K.; Figueroa, J. S. Solution Dynamics of Redox Noninnocent Nitrosoarene Ligands: Mapping the Electronic Criteria for the Formation of Persistent Metal-Coordinated Nitroxide Radicals. *Inorg. Chem.* **2015**, *54* (14), 7110−7121.
(18) Kundu, S.; Stieber, S. C. E.; Ferrier, M. G.; Kozimor, S. A.; Bertke, J. A.; Warren, T. H. Redox Non-Innocence of Nitrosobenzene at Nickel. *Angew. Chem., Int. Ed.* **2016**, *55* (35), 10321−10325.
(19) Effaty, F.; Zsombor-Pindera, J.; Kazakova, A.; Girard, B.; Askari, M. S.; Ottenwaelder, X. Ligand and electronic effects on copper-arylnitroso self-assembly. *New J. Chem.* **2018**, *42* (10), 7758−7764.
(20) Ferretti, E.; Dechert, S.; Meyer, F. Reductive Binding and Ligand-Based Redox Transformations of Nitrosobenzene at a Dinickel(II) Core. *Inorg. Chem.* **2019**, *58* (8), 5154−5162.
(21) Dey, S.; Panda, S.; Ghosh, P.; Lahiri, G. K. Electronically Triggered Switchable Binding Modes of the C-Organonitroso (ArNO) Moiety on the {Ru(acac)$_2$} Platform. *Inorg. Chem.* **2019**, *58* (2), 1627−1637.
(22) Chan, S.-C.; Wong, C.-Y. Recent developments in ruthenium-nitrosoarene chemistry: Unconventional synthetic strategies, new ligand designs, and exploration of ligands redox non-innocence. *Coord. Chem. Rev.* **2020**, *402*, 213082.
(23) Askari, M. S.; Effaty, F.; Gennarini, F.; Orio, M.; Le Poul, N.; Ottenwaelder, X. Tuning Inner-Sphere Electron Transfer in a Series of Copper/Nitrosoarene Adducts. *Inorg. Chem.* **2020**, *59* (13), 8678−8689.
(24) Solomon, E. I.; Brunold, T. C.; Davis, M. I.; Kemsley, J. N.; Lee, S.-K.; Lehnert, N.; Neese, F.; Skulan, A. J.; Yang, Y.-S.; Zhou, J. Geometric and Electronic Structure/Function Correlations in Non-Heme Iron Enzymes. *Chem. Rev.* **2000**, *100* (1), 235−350.
(25) Solomon, E. I.; Heppner, D. E.; Johnston, E. M.; Ginsbach, J. W.; Cirera, J.; Qayyum, M.; Kieber-Emmons, M. T.; Kjaergaard, C. H.; Hadt, R. G.; Tian, L. Copper Active Sites in Biology. *Chem. Rev.* **2014**, *114* (7), 3659−3853.
(26) Elwell, C. E.; Gagnon, N. L.; Neisen, B. D.; Dhar, D.; Spaeth, A. D.; Yee, G. M.; Tolman, W. B. Copper-Oxygen Complexes Revisited: Structures, Spectroscopy, and Reactivity. *Chem. Rev.* **2017**, *117* (3), 2059−2107.
(27) Trammell, R.; Rajabimoghadam, K.; Garcia-Bosch, I. Copper-Promoted Functionalization of Organic Molecules: from Biologically Relevant Cu/O_2 Model Systems to Organometallic Transformations. *Chem. Rev.* **2019**, *119* (4), 2954−3031.
(28) Askari, M. S.; Esguerra, K. V. N.; Lumb, J.-P.; Ottenwaelder, X. A Biomimetic Mechanism for the Copper-Catalyzed Aerobic Oxygenation of 4-tert-Butylphenol. *Inorg. Chem.* **2015**, *54* (17), 8665−8672.
(29) Fokin, S. V.; Romanenko, G. V.; Ovcharenko, V. I. The first metal complex with a vic-dihydroxyamine and its oxidised derivative. *Mendeleev Commun.* **2001**, *11* (4), 127−128.
(30) McCauley, K. M.; Wilson, S. R.; van der Donk, W. A. Dichloroacetylene Is Not the Precursor to Dichlorinated Vinylcobaloxime and Vinylcobalamin in Cobalt Catalyzed Dechlorination of Perchloro- and Trichloroethylene. *Inorg. Chem.* **2002**, *41* (22), 5844−5848.
(31) Luzyanin, K. V.; Gushchin, P. V.; Pombeiro, A. J. L.; Haukka, M.; Ovcharenko, V. I.; Kukushkin, V. Y. Oxidation of Pt-bound Bis-hydroxylamine as a Novel Route to Unexplored Dinitrosoalkane Ligated Species. *Inorg. Chem.* **2008**, *47* (15), 6919−6930.
(32) Alluisetti, G. E.; Almaraz, A. E.; Amorebieta, V. T.; Doctorovich, F.; Olabe, J. A. Metal-Catalyzed Anaerobic Disproportionation of Hydroxylamine. Role of Diazene and Nitroxyl Intermediates in the Formation of N_2, N_2O, NO^+, and NH_3. *J. Am. Chem. Soc.* **2004**, *126* (41), 13432−13442.
(33) Gutiérrez, M. M.; Alluisetti, G. B.; Olabe, J. A.; Amorebieta, V. T. Catalytic disproportionation of N-alkylhydroxylamines bound to pentacyanoferrates. *Dalton Trans.* **2009**, No. 7, 1187−1194.
(34) Williams, K. D.; Cardenas, A. J. P.; Oliva, J. D.; Warren, T. H. Copper C-Nitroso Compounds: Activation of Hydroxylamines and NO Reactivity. *Eur. J. Inorg. Chem.* **2013**, *2013* (22−23), 3812−3816.
(35) *The Chemistry of Hydroxylamines, Oximes and Hydroxamic Acids*; Rappoport, Z.; Liebman, J. F., Eds.; John Wiley & Sons Ltd.: Chichester, UK, 2009; Vol. *1*.
(36) Gordon, J. B.; Vilbert, A. C.; DiMucci, I. M.; MacMillan, S. N.; Lancaster, K. M.; Moënne-Loccoz, P.; Goldberg, D. P. Activation of Dioxygen by a Mononuclear Nonheme Iron Complex: Sequential Peroxo, Oxo, and Hydroxo Intermediates. *J. Am. Chem. Soc.* **2019**, *141* (17), 7046−7055.
(37) Walroth, R. C.; Miles, K. C.; Lukens, J. T.; MacMillan, S. N.; Stahl, S. S.; Lancaster, K. M. Electronic Structural Analysis of Copper(II)-TEMPO/ABNO Complexes Provides Evidence for Copper(I)-Oxoammonium Character. *J. Am. Chem. Soc.* **2017**, *139* (38), 13507−13517.
(38) Usman, M.; Zhang, X.-W.; Wu, D.; Guan, Z.-H.; Liu, W.-B. Application of dialkyl azodicarboxylate frameworks featuring multifunctional properties. *Org. Chem. Front.* **2019**, *6* (11), 1905−1928.
(39) Wang, D.; Leng, X.; Ye, S.; Deng, L. The structure contains a small component of a complex with a Ar-Cl bond instead of the ArNO, suggesting C-NO bond cleavage followed by Cl rebound. Such C-NO bond cleavage was shown to occur with Co(O). *J. Am. Chem. Soc.* **2019**, *141*, 7731−7735.
(40) Baker, M. L.; Mara, M. W.; Yan, J. J.; Hodgson, K. O.; Hedman, B.; Solomon, E. I. K- and L-edge X-ray absorption spectroscopy (XAS) and resonant inelastic X-ray scattering (RIXS) determination of differential orbital covalency (DOC) of transition metal sites. *Coord. Chem. Rev.* **2017**, *345*, 182−208.
(41) DiMucci, I. M.; MacMillan, S. N.; Walroth, R. C.; Lancaster, K. M. Scrutinizing "Ligand Bands" via Polarized Single-Crystal X-ray Absorption Spectra of Copper(I) and Copper(II) Bis-2,2′-bipyridine Species. *Inorg. Chem.* **2020**, *59* (18), 13416−13426.
(42) Markó, I. E.; Gautier, A.; Dumeunier, R.; Doda, K.; Philippart, F.; Brown, S. M.; Urch, C. J. Efficient, Copper-Catalyzed, Aerobic Oxidation of Primary Alcohols. *Angew. Chem., Int. Ed.* **2004**, *43* (12), 1588−1591.
(43) McCann, S. D.; Stahl, S. S. Mechanism of Copper/Azodicarboxylate-Catalyzed Aerobic Alcohol Oxidation: Evidence for Uncooperative Catalysis. *J. Am. Chem. Soc.* **2016**, *138* (1), 199−206.
(44) Ryland, B. L.; McCann, S. D.; Brunold, T. C.; Stahl, S. S. Mechanism of Alcohol Oxidation Mediated by Copper(II) and Nitroxyl Radicals. *J. Am. Chem. Soc.* **2014**, *136* (34), 12166−12173.
(45) McCann, S. D.; Lumb, J.-P.; Arndtsen, B. A.; Stahl, S. S. Second-Order Biomimicry: In Situ Oxidative Self-Processing Converts Copper(I)/Diamine Precursor into a Highly Active Aerobic Oxidation Catalyst. *ACS Cent. Sci.* **2017**, *3* (4), 314−321.
(46) Sinha, S.; Das, S.; Sikari, R.; Parua, S.; Brandaõ, P.; Demeshko, S.; Meyer, F.; Paul, N. D. Redox Noninnocent Azo-Aromatic Pincers and Their Iron Complexes. Isolation, Characterization, and Catalytic Alcohol Oxidation. *Inorg. Chem.* **2017**, *56* (22), 14084−14100.
(47) Bezdek, M. J.; Guo, S.; Chirik, P. J. Terpyridine Molybdenum Dinitrogen Chemistry: Synthesis of Dinitrogen Complexes That Vary by Five Oxidation States. *Inorg. Chem.* **2016**, *55* (6), 3117−3127.

https://dx.doi.org/10.1021/jacs.0c09300
J. Am. Chem. Soc. XXXX, XXX, XXX−XXX

(48) Annibale, V. T.; Song, D. Multidentate actor ligands as versatile platforms for small molecule activation and catalysis. *RSC Adv.* **2013**, *3* (29), 11432−11449.
(49) Kaim, W.; Beyer, K.; Filippou, V.; Záliš, S. Charge and spin coupling in copper compounds with hemilabile noninnocent ligands - Ambivalence in three dimensions. *Coord. Chem. Rev.* **2018**, *355*, 173−179.
(50) Storr, T.; Mukherjee, R. Preface for the Forum on Applications of Metal Complexes with Ligand-Centered Radicals. *Inorg. Chem.* **2018**, *57* (16), 9577−9579.
(51) Que, L.; Tolman, W. B. Biologically inspired oxidation catalysis. *Nature* **2008**, *455* (7211), 333−340.
(52) Smith, M. A.; Majer, S. H.; Vilbert, A. C.; Lancaster, K. M. Controlling a burn: outer-sphere gating of hydroxylamine oxidation by a distal base in cytochrome P460. *Chem. Sci.* **2019**, *10* (13), 3756−3764.
(53) Chirik, P. J.; Wieghardt, K. Radical Ligands Confer Nobility on Base-Metal Catalysts. *Science* **2010**, *327* (5967), 794−795.

https://dx.doi.org/10.1021/jacs.0c09300
J. Am. Chem. Soc. XXXX, XXX, XXX−XXX